# Toluene internal-rotation: Measurement and simulation of the high-resolution $S_1-S_0$ fluorescence excitation spectrum at 0.5 K

Allan L. L. East, Haisheng Liu, and Edward C. Lim[a)]
*Department of Chemistry, University of Akron, Akron, Ohio 44325-3601*

Per Jensen
*FB 9, Theoretische Chemie, Bergische Universität-Gesamthochschule Wuppertal, D-42097 Wuppertal, Germany*

Isabelle Déchène, Marek Z. Zgierski, Willem Siebrand, and P. R. Bunker
*Steacie Institute for Molecular Sciences, National Research Council of Canada, Ottawa, Ontario, Canada K1A 0R6*

(Received 11 August 1999; accepted 8 October 1999)

Rotational structure in the origin band of the $S_1-S_0$ fluorescence excitation spectrum of toluene has been measured at 0.012 $cm^{-1}$ resolution with a rotational temperature of 0.5 K using a pulsed beam apparatus. Such spectra have been obtained for the parent isotopomer and for the isotopomers with mono- and di-deuterated methyl groups. These, and previously known forbidden bands in which the internal-rotation quantum number $K_i$ changes, are simulated here using *ab initio* internal-rotation-angle-dependent geometries, potential functions, and electronic transition moment function. An adjustment of some of the *ab initio* parameters allows a close fitting of the spectra to be made, and this can only be achieved if bond lengths and angles are allowed to vary with internal rotation. The resulting geometries for ground and excited-state toluene are the most accurate to date.
 [S0021-9606(00)01601-9]

## I. INTRODUCTION

Toluene ($C_6H_5CH_3$) is a readily available prototype for studying the effects of nearly-free internal-rotation of a methyl group. The methyl group internal-rotation potential in the torsional angle $\rho$ can be written

$$V(\rho)=(V_6/2)(1-\cos 6\rho), \tag{1}$$

and there is a small barrier height $|V_6|$ that has been determined to be 4.9 $cm^{-1}$ for the $S_0$ ground state[1] and 25 $cm^{-1}$ for the $S_1$ excited state.[2] The effect of the internal rotation in toluene can be studied using ultraviolet, infrared, Raman, and microwave spectroscopy techniques. In this work we study the fluorescence excitation spectrum of the $S_1-S_0$ transition. We obtain the origin band (having $\Delta K_i=0$, where $K_i$ is the internal-rotation quantum number) with partial rotational resolution for the parent ($d_0$) isotopomer and for the methyl mono- and di-deuterated ($d_1$ and $d_2$) isotopomers. With the help of some *ab initio* calculations, we analyze these spectra, and existing spectra of other bands, to determine the internal-rotation dependence of the geometrical parameters, potential energy, and electronic transition moment.

The $S_1-S_0$ electronic transition is allowed in toluene although it is weak; the analogous transition in benzene is forbidden. Forbidden bands involving changes in internal rotor state are seen in the toluene $S_1-S_0$ fluorescence excitation and dispersed fluorescence, and assignments were reported in 1981 by Murakami, Ito, and Kaya.[3] They obtained the excitation spectrum using resonance-enhanced multiphoton ionization (REMPI) and a supersonic jet expansion. The most intense of these bands, $(K_i'-K_i'')=(3-0)$ and $(0-3)$, could be seen in previous fluorescence excitation and dispersed fluorescence spectra by Smalley and co-workers[4,5] but they were not assigned. In 1987, Breen, Warren, Bernstein, and Seeman[2] reported the internal-rotation energy levels of the $S_0$ and $S_1$ states of toluene as determined from REMPI and dispersed emission. Their modeling provided values for the $V_6$ barrier heights of both states, but not the sign of $V_6$ for the $S_0$ state.[6] In 1995, Weisshaar and co-workers[7] reported REMPI spectra for toluene and five similar molecules, and presented a model for the intensities of the internal-rotation bands which (i) demonstrates that the transition dipole moment varies with internal-rotation, and (ii) agrees with the $G_{12}$-symmetry selection rules used previously.[2,8] In 1997 Siebrand, Lim, and co-workers[9] extended the studies to toluene with a mono- or di-deuterated methyl group, and demonstrated excellent agreement with a model that incorporated *ab initio* zero point energy contributions to the internal-rotation potential. These contributions, from the $\rho$-dependence of the frequencies of the $3N-7=38$ small amplitude vibrations, resulted in internal-rotation potentials of the form

$$V(\rho)=(V_2/2)(1-\cos 2\rho)+(V_4/2)(1-\cos 4\rho)+(V_6/2)(1-\cos 6\rho) \tag{2}$$

with dominant $V_2$ terms for the mono- and di-deuterated methyl rotors.

Studies of the rotational structure have been more limited. The only reported microwave (pure rotation) studies are

[a)]Holder of the Goodyear Chair in Chemistry of the University of Akron.

 

the papers of Rudolph and co-workers.[1,10] They determined rotational constants, and the $|V_6|$ barrier height for undeuterated and partially deuterated isotopomers.

In infrared and Raman studies, there has been measurement and modeling of the band envelopes for C–H and C–D stretching fundamentals and overtones of various toluenes, by Cavagnat and co-workers,[11,12] Henry and co-workers,[13–15], Ghosh and co-workers,[16] and Anastasakos and Wildman.[17] Cavagnat and co-workers in particular have been able to demonstrate improvements in the fitting to band contours by using twofold barrier terms for partially deuterated methyl groups in toluene[11,12] and nitromethane.[18,19]

In contrast to the vibrational spectra studies, some rotational structure has been observed in the $S_1-S_0$ spectra. In 1971, Cvitaš and Hollas[20] reported the first $S_1-S_0$ spectrum of a toluene system with partial rotational resolution. They obtained a room-temperature ultraviolet absorption spectrum of the origin band of *p*-fluorotoluene, and analyzed their results assuming free internal-rotation of the methyl group. In 1982-83, Seliskar and Leugers[21–23] examined the $S_1-S_0$ origin band of toluene, first fitting to the band contour at room-temperature[21] and supersonic-jet temperatures,[22] and then fitting a higher-resolution supersonic-jet spectrum.[23] They modeled the rotational structure using a free internal-rotor Hamiltonian. In 1993, Ishikawa, Kajimoto, and Kato[24] obtained fluorescence excitation spectra for the $S_1-S_0$ transition in phenylsilane, $C_6H_5SiH_3$, with sufficient resolution to see some rotational features on the origin and 3–0 bands. They modeled the rotational structure with a simple free internal-rotor Hamiltonian with inclusion of an off-diagonal rotation-torsion coupling term.

Here we present measurements of the rotational structure of the origin band for the $d_0$, $d_1$, and $d_2$ isotopomers of toluene, together with our simulations of these spectra. This work was motivated by the desire to address the discrepancies previously observed in the fitting of the $S_1-S_0$ internal-rotation structure, and to provide a model that more accurately describes and simulates the rotation and internal-rotation degrees of freedom in toluene.

## II. EXPERIMENT

The description of our experimental apparatus has been given before.[25] Only a brief overview will be given here. The supersonic jet apparatus was of conventional design. The directions of laser, jet, and fluorescence collection are mutually perpendicular. The excitation source for the fluorescence excitation spectrum was a Fourier-transform-limited (FTL) laser system. It was a pulse-amplified CW ring dye laser (Coherent 699-29) pumped with an argon ion laser (Coherent innova 200-15) and operated with pyrromethane-556 dye. The pulse amplifier (Lambda Physik FL2003) was pumped by the second harmonic of an excimer (Lambda Physik COMPEX 102). The output of the pulse-amplified single-mode laser, of 90 MHz linewidth, was frequency doubled into the near ultraviolet. Absolute calibration of the spectra was performed by simultaneously recording the iodine spectrum using the fundamental of the ring dye laser. A slit aperture oriented parallel to the jet direction was mounted in front of the PMT (Hamamatsu 1527P) to reduce the Doppler width. Helium was passed through the sample reservoir and the gas mixture was expanded into vacuum through a 0.8 mm pulsed pinhole nozzle (General Valve). The cooling conditions were adjusted by varying helium pressure from 40 to 80 psi and sample temperature from $-30\,^{\circ}\mathrm{C}$ to room temperature. The fluorescence was collected by a PMT after passing an optical filter (Hoya Optics UV-30).

The methods of sample preparation of toluene-$d_1$ ($\alpha$-deuterotoluene) and toluene-$d_2$ ($\alpha$-dideuterotoluene) have been described before.[9]

## III. THEORY

In order to simulate the spectrum from first principles, we must (a) Calculate the geometry and potential energy for internally rotating toluene in both electronic states, (b) Calculate the resulting rotation-torsion energies and wave functions for both electronic states, and (c) Calculate the line positions and relative intensities for rotation-torsion transitions between the two states.

### A. Geometry and potential energy

We performed complete-active-space self-consistent field (CASSCF) (Refs. 26,27) geometry optimizations of both the $S_0$ and $S_1$ states at two methyl group conformations (eclipsed and staggered). We used the GAUSSIAN 94 (Ref. 28) program system with the 6-31G$(d,p)$ basis set and an active space of the six phenyl $\pi$ electrons in the six $\pi$ and $\pi^*$ orbitals. We derived formulas for the values of the coordinates along the torsional minimum energy path (MEP) that connects the optimized eclipsed and staggered geometries. These $\rho$-dependent MEP coordinates are given in Table I, with the atom numbering scheme of Fig. 1. The torsional angle $\rho$ is defined as the average of the six dihedral angles between methyl group CH bonds and the bonds $C_1C_2$ and $C_1C_6$. Due to symmetry relations such as

$$R_{1,6}(\rho)=R_{1,2}(\rho+\pi) \tag{3}$$

and

$$\theta_{14,12,1}(\rho)=\theta_{13,12,1}(\rho+2\pi/3), \tag{4}$$

where, for example, $\theta_{14,12,1}$ is the angle between bonds $H_{14}C_{12}$ and $C_{12}C_1$, we do not have to include all bond lengths and angles in Table I. Also for fitting to the rotational structure in the spectrum it is helpful to use the distance $R_{1,4}$, rather than $R_{2,3}$ and $R_{5,6}$; these two can be obtained from the tabulated bond lengths and angles. The angle $\tau_{13,12,1,2}$ is the dihedral angle $H_{13}C_{12}C_1C_2$, and the angle $\beta_{13,12,1}$ is $\pi-\theta_{13,12,1}$. The angles $\gamma$ and $\delta$ are the in-plane and out-of-plane components (respectively) of $\pi-\theta_{12,1,4}$; they determine the ''tilt'' of the methyl group relative to $R_{1,4}$.

The torsional potential energy parameters $V_2$, $V_4$, and $V_6$ in Eqs. (1) and (2) were obtained from the CASSCF electronic energies supplemented by the $\rho$-dependence of the sum of the zero point energies of the 38 small-amplitude vibrational modes. The zero point energy sum was computed as half the sum of the 38 CASSCF harmonic frequencies for each isotopomer. These parameters are given in Table II. Inclusion of the zero point energy sum of the high frequency

TABLE I. Geometries for ground- and excited-state toluene, from *ab initio* (CASSCF)[a] and least-squares-fitting (LSQ), using two different internal rotation models.[b]

| Parameters[c] | $S_0$ state (CASSCF) | $S_0$ state (I, LSQ) | $S_0$ state (II, LSQ) | $S_1$ state (CASSCF) | $S_1$ state (I, LSQ) | $S_1$ state (II, LSQ) |
|---|---|---|---|---|---|---|
| $R_{1,2}$ | 1.4000 $-0.0027\cos 3\rho$ | 1.3964 | 1.3966 $-0.0027\cos 3\rho$ | 1.4387 $+0.0004\cos 3\rho$ | 1.4388 | 1.4391 $+0.0004\cos 3\rho$ |
| $R_{3,4}$ | 1.3951 $-0.0022\cos 3\rho$ | 1.3915 | 1.3917 $-0.0022\cos 3\rho$ | 1.4320 $+0.0003\cos 3\rho$ | 1.4321 | 1.4324 $+0.0003\cos 3\rho$ |
| $R_{1,4}$ | 2.8160 | 2.8168 | 2.8177 | 2.88555 | 2.8778 | 2.8755 |
| $R_{1,12}$ | 1.51185 | 1.5123 | 1.5128 | 1.5038 | 1.4997 | 1.4985 |
| $R_{2,7}$ | 1.0769 | 1.084 | 1.084 | 1.0744 | 1.084 | 1.084 |
| $R_{3,8}$ | 1.0760 | 1.084 | 1.084 | 1.0737 | 1.084 | 1.084 |
| $R_{4,9}$ | 1.0757 | 1.084 | 1.084 | 1.0737 | 1.084 | 1.084 |
| $R_{12,13}$ | 1.0854 | 1.1002 | 1.0972 | 1.0865 | 1.1095 | 1.0985 |
| | $-0.0014\cos 2\rho$ | | $-0.0014\cos 2\rho$ | $-0.0024\cos 2\rho$ | | $-0.0024\cos 2\rho$ |
| $\theta_{2,1,6}$ | 118.32 | 117.82 | 117.85 | 118.66 | 118.68 | 118.72 |
| $\theta_{3,4,5}$ | 119.48 | 118.98 | 119.00 | 119.82 | 119.84 | 119.88 |
| $\theta_{7,2,1}$ | 119.53 | 119.53 | 119.53 | 119.56 | 119.56 | 119.56 |
| $\theta_{8,3,4}$ | 120.08 | 120.08 | 120.08 | 120.07 | 120.07 | 120.07 |
| $\beta_{13,12,1}$ | 68.79 | 70.83 | 70.43 | 68.69 | 71.87 | 70.33 |
| | $-0.013\cos 2\rho$ | | $-0.013\cos 2\rho$ | $-0.11\cos 4\rho$ | | $-0.11\cos 4\rho$ |
| $\gamma$ | $0.54\cos 3\rho$ | 0 | $0.54\cos 3\rho$ | $0.63\cos 3\rho$ | 0 | $0.54\cos 3\rho$ |
| $\delta$ | $-1.26\sin 3\rho$ | 0 | $-1.26\sin 3\rho$ | $-2.94\sin 3\rho$ | 0 | $-2.5\sin 3\rho$ |
| $\tau_{13,12,1,2}$ | $\rho-0.20\sin\rho$ | $\rho$ | $\rho-0.20\sin\rho$ | $\rho-0.26\sin\rho$ | $\rho$ | $\rho-0.26\sin\rho$ |

[a]From CASSCF(6,6)/6-31G(d,p) optimizations.
[b]Model I is the simple $C_{2v}$–$C_{3v}$ model, and Model II is the minimum energy path model.
[c]Distances in Å and angles in deg. The coordinates are defined by Fig. 1. $\beta_{13,12,1}$ is $\pi-\theta_{13,12,1}$, $\gamma$ and $\delta$ are in-plane and out-of-plane components (respectively) of $\pi-\theta_{12,1,4}$, and $\tau_{13,12,1,2}$ is a dihedral angle. Other coordinates are related by symmetry, e.g., $\theta_{14,12,1}(\rho)=\theta_{13,12,1}(\rho+2\pi/3)$ and $R_{1,6}(\rho)=R_{1,2}(\rho+\pi)$.

vibrations has a small effect on the $V_6$ barrier term in each electronic state. The purely electronic value of $V_6$ is calculated to be $-1.8$ cm$^{-1}$ for the $S_0$ state and $-22.6$ cm$^{-1}$ for the $S_1$ state. The $-$ sign indicates that the equilibrium structure is staggered with a symmetry plane bisecting the phenyl ring.

The CASSCF calculation predicts that the $S_1-S_0$ transition energy ($T_0$) for toluene-$d_0$ is 37 160 cm$^{-1}$($T_e$ = 38 300 cm$^{-1}$); our experimental value for $T_0$ is 37 476.56 cm$^{-1}$.

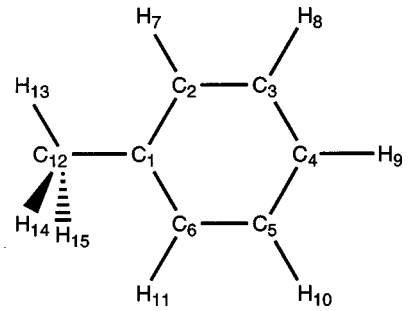


FIG. 1. Diagram of the $\rho=0$ (eclipsed) conformation of toluene, with our atom numbering convention.

### B. Energies and wave functions

The generalized rotation-contortion Hamiltonian,[29] which allows for the coupling of a contortional mode with overall rotation, was used to determine the rotation-torsion energies $\epsilon_{\rm rt}$ and wave functions $\Phi_{\rm rt}$. We diagonalize the matrix representation of this Hamiltonian in a basis of product functions, so that the eigenfunctions are given by

$$\Phi_{\rm rt}=\sum_{j,k} c_{jk}\,\Phi_{J,k}\Phi_j, \tag{5}$$

where the $c_{jk}$ are eigenvector coefficients. The rotational $\Phi_{J,k}$ functions are Szalay-Lane linear combinations of symmetric top functions,[30] while the torsional $\Phi_j$ functions are free internal-rotor functions given by

$$\Phi_{\rm tor}^{(K_i,\pm)}=\Phi_j=[\exp(iK_i\rho)\pm\exp(-iK_i\rho)]/(2\sqrt{\pi}), \tag{6}$$

TABLE II. Internal rotation potential energy parameters ($cm^{-1}$).

| State | Method | Isotopomer | $V_2$ | $V_4$ | $V_6$ |
|---|---|---|---|---|---|
| $S_0$ | CASSCF | $d_0$(PhCH$_3$) | ··· | ··· | −3.0 |
| | | $d_1$(PhCH$_2$D) | 14.2 | 0.1 | −2.8 |
| | | $d_2$(PhCHD$_2$) | −12.6 | 0.0 | −2.8 |
| | | $d_3$(PhCD$_3$) | ··· | ··· | −2.9 |
| | I, LSQ | $d_0$(PhCH$_3$) | ··· | ··· | −3.0[a] |
| | | $d_1$(PhCH$_2$D) | 23.2 | 0.0[a] | −2.9[a] |
| | | $d_2$(PhCHD$_2$) | −26.6 | 0.0[a] | −2.8[a] |
| | | $d_3$(PhCD$_3$) | ··· | ··· | −2.8[a] |
| | II, LSQ | $d_0$ (PhCH$_3$) | ··· | ··· | −3.0[a] |
| | | $d_1$ (PhCH$_2$D) | 23.8 | 0.0[a] | −2.9[a] |
| | | $d_2$ (PhCHD$_2$) | −26.0 | 0.0[a] | −2.8[a] |
| | | $d_3$(PhCD$_3$) | ··· | ··· | −2.8[a] |
| $S_1$ | CASSCF | $d_0$ (PhCH$_3$) | ··· | ··· | −23.4 |
| | | $d_1$ (PhCH$_2$D) | 21.3 | −0.5 | −22.4 |
| | | $d_2$ (PhCHD$_2$) | −19.4 | 0.7 | −21.9 |
| | | $d_3$(PhCD$_3$) | ··· | ··· | −21.7 |
| | I, LSQ | $d_0$ (PhCH$_3$) | ··· | ··· | −25.8 |
| | | $d_1$ (PhCH$_2$D) | 37.2 | 0.0[a] | −24.7[b] |
| | | $d_2$ (PhCHD$_2$) | −34.5 | 0.0[a] | −24.2[b] |
| | | $d_3$(PhCD$_3$) | ··· | ··· | −23.9[b] |
| | II, LSQ | $d_0$ (PhCH$_3$) | ··· | ··· | −25.5 |
| | | $d_1$ (PhCH$_2$D) | 37.0 | 0.0[a] | −24.4[b] |
| | | $d_2$ (PhCHD$_2$) | −34.1 | 0.0[a] | −23.9[b] |
| | | $d_3$(PhCD$_3$) | ··· | ··· | −23.6[b] |

[a]Held fixed in all fittings.
[b]Constrained using Eq. (A1).

where the index $j$ denotes both the $\pm$ and the $K_i$ value. Since the internal-rotation barriers are very low, and the dependencies of the bond lengths and other bond angles on the torsional angle are weak, the eigenvectors will be dominated by either one or a symmetric pair of basis function products. As a result the quantum numbers $K$ and $K_i$ will be useful energy level, and selection rule, labels.

In the Hamiltonian[29] the $\rho$-dependent coefficients are computed directly from Cartesian coordinates (not rotational constants), assuming a model for the internal-rotation path. We considered two such models; Model I, a traditional simple model with rigid $C_{3v}-C_{2v}$ methyl-phenyl groups, and Model II, a minimum energy path model in which the geometrical parameters were allowed to vary with $\rho$. We began with the CASSCF parameter values, and in the fitting procedure these values were adjusted; the fitting details appear in the Appendix.

### C. Intensities

The principal quantity in the intensity calculation is the line strength for each rovibronic transition, which we write as (see Sec. 14.1 of Ref. 31),

$$S(f\leftarrow i)=g_{\rm ns}\times\sum_{m',m''}\sum_{A=\xi\eta\zeta}\left|\langle\Phi'_{\rm rt}\Phi'_{\rm vib}\Phi^{(S_1)}_{\rm elec}|\mu_A|\Phi''_{\rm rt}\Phi''_{\rm vib}\Phi^{(S_0)}_{\rm elec}\rangle\right|^2, \quad (7)$$

for a transition between an initial rovibronic state $i$ and a final state $f$, where $g_{\rm ns}$ is the nuclear spin statistical weight

TABLE III. Parameters varied during the spectral fitting.

| | | | | Parameters varied | | |
|---|---|---|---|---|---|---|
| State | parameter[a] | Model I | Model I | 1st fit[b] | 2nd fit[c] | 3rd fit[d] |
| | $\nu_{\rm origin}(d_0)$ | 37 476.57 | 37 476.56 | | ● | |
| | $\nu_{\rm origin}(d_1)$ | 37 479.84 | 37 479.84 | | ● | |
| | $\nu_{\rm origin}(d_2)$ | 37 487.33 | 37 487.33 | | ● | |
| $S_1$ | $V_2$ ($d_1$) | 37.2 | 37.0 | ● | | ● |
| | $V_2$ ($d_2$) | −34.5 | −34.1 | ● | | ● |
| | $V_6$ ($d_0$) | −25.8 | −25.5 | ● | | |
| | $K_T$ | ··· | 0.8514 | ●[e] | ●[e] | |
| | $K_M$ | 1.0463 | 1.0239 | ● | ● | |
| | $K_P$ | 1.0002 | 1.0005 | | ● | |
| | $K_R$ | 0.9973 | 0.9965 | | ● | |
| $S_0$ | $V_2$ ($d_1$) | 23.2 | 23.8 | ● | | ● |
| | $V_2$ ($d_2$) | −26.6 | −26.0 | ● | | ● |
| | $K_M$ | 1.0297 | 1.0238 | ● | | |
| | $K_P$ | 0.9958 | 0.9960 | | ● | |
| | $K_R$ | 1.0003 | 1.0006 | | ● | |

[a]$V_n$ and $\nu_{\rm origin}$ are in $cm^{-1}$, and the $K$ scaling parameters are dimensionless.
[b]Fitting to internal-rotation structure.
[c]Fitting to rotational structure.
[d]Final fitting to internal-rotation structure.
[e]Parameter varied only in Model II fits.

(we presume that nuclear hyperfine structure is unresolved), $m'$ and $m''$ are the quantum numbers for the space-fixed components of the total angular momentum $J$, and $\mu_A$ ($A=\xi$, $\eta$, or $\zeta$) is a space fixed component of the electric dipole moment operator. Substituting Eq. (5) into this equation for the $S_0$ and $S_1$ electronic states we obtain the expression for the dipole moment matrix element as

$$\langle\Phi'_{\rm rt}\Phi'_{\rm vib}\Phi^{(S_1)}_{\rm elec}|\mu_A|\Phi''_{\rm rt}\Phi''_{\rm vib}\Phi^{(S_0)}_{\rm elec}\rangle = \sum_{j',k',j'',k''}(c_{j'k'})^*c_{j''k''}\times\langle\Phi_{J',k'}\Phi_{j'}\Phi'_{\rm vib}\Phi^{(S_1)}_{\rm elec}|\mu_A|\Phi_{J'',k''}\Phi_{j''}\Phi''_{\rm vib}\Phi^{(S_0)}_{\rm elec}\rangle. \quad (8)$$

Expressing $\mu_A$ in terms of the molecule fixed $abc$ components $\mu_\alpha$, and the direction cosine matrix elements $\lambda_{\alpha A}$, and separating the rotational and vibronic integrals, we can rewrite Eq. (8) as

$$\langle\Phi'_{\rm rt}\Phi'_{\rm vib}\Phi^{(S_1)}_{\rm elec}|\mu_A|\Phi''_{\rm rt}\Phi''_{\rm vib}\Phi^{(S_0)}_{\rm elec}\rangle = \sum_{j',k',j'',k''}(c_{j'k'})^*c_{j''k''}\times\sum_{\alpha=abc}\langle\Phi_{J',k'}|\lambda_{\alpha A}|\Phi_{J'',k''}\rangle\times\langle\Phi_{j'}\Phi'_{\rm vib}\Phi^{(S_1)}_{\rm elec}|\mu_\alpha|\Phi_{j''}\Phi''_{\rm vib}\Phi^{(S_0)}_{\rm elec}\rangle. \quad (9)$$

Electronic and vibrational variables are separated by writing

$$\langle\Phi_{j'}\Phi'_{\rm vib}\Phi^{(S_1)}_{\rm elec}|\mu_\alpha|\Phi_{j''}\Phi''_{\rm vib}\Phi^{(S_0)}_{\rm elec}\rangle = \langle\Phi_{j'}\Phi'_{\rm vib}|\mu_\alpha(S_1,S_0)|\Phi_{j''}\Phi''_{\rm vib}\rangle, \quad (10)$$

where $\mu_\alpha(S_1,S_0)$ is the electronic transition moment $\langle\Phi^{(S_1)}_{\rm elec}|\mu_\alpha|\Phi^{(S_0)}_{\rm elec}\rangle$, and we expand it as

$$\mu_\alpha(S_1,S_0)=\mu_\alpha^{(0)}(S_1,S_0;\rho)+\sum_r \mu_\alpha^{(r)}(S_1,S_0;\rho)Q_r + \frac{1}{2}\sum_{r,s}\mu_\alpha^{(r,s)}(S_1,S_0;\rho)Q_rQ_s+\cdots, \quad (11)$$

where $r$ and $s = 1$ to 38 for toluene. Neglecting the dependence of the electronic transition moment on the 38 small amplitude vibrations Eq. (9) becomes

$$\langle \Phi'_{\rm rt}\Phi'_{\rm vib}\Phi^{(S_1)}_{\rm elec}|\mu_A|\Phi''_{\rm rt}\Phi''_{\rm vib}\Phi^{(S_0)}_{\rm elec}\rangle = \sum_{j',k',j'',k''}(c_{j'k'})^* c_{j''k''}\sum_{\alpha=abc}\langle\Phi_{J',k'}|\lambda_{\alpha A}|\Phi_{J'',k''}\rangle \times\langle\Phi_{j'}|\mu_\alpha^{(0)}(S_1,S_0;\rho)\langle\Phi'_{\rm vib}|\Phi''_{\rm vib}\rangle|\Phi_{j''}\rangle. \quad (12)$$

The vibrational overlap factor $\langle\Phi'_{\rm vib}|\Phi''_{\rm vib}\rangle$ is the same for all the transitions we consider, and so it can be ignored in the calculation of relative intensities.

In practice, we calculate the line strengths by changing to irreducible spherical tensor operator notation as explained in Sec. 14.1.3 of Ref. 32. Instead of the molecule fixed $abc$ components $\mu_\alpha$ of the dipole moment, we use the linear combinations,

$$\mu_{\rm m}^{(1,\pm1)}=[\mp\mu_b+i\mu_c]/\sqrt{2}$$

and

$$\mu_{\rm m}^{(1,0)}=\mu_a. \quad (13)$$

The expression for the line strength is straightforwardly obtained from Eqs. (14)–(43) and (14)–(44) of Ref. 32. We have to make allowance for the facts that we consider two different electronic states but only one vibration, the torsion, and that the rotational basis functions used are not the symmetric top functions $|J,k,m\rangle$, but linear combinations of them. We obtain

$$S(f\leftarrow i)=g_{\rm ns}\left|\sum_{j',j''}\sum_{k'=-J'}^{J'}\sum_{k''=-J''}^{J''}(c_{j'k'})^* c_{j''k''}M^{(S_1J'j'k')}_{(S_0J''j''k'')}\right|^2, \quad (14)$$

where

$$M^{(S_1J'j'k')}_{(S_0J''j''k'')}=(-1)^{J'+J''+k'}\sqrt{(2J''+1)(2J'+1)}\sum_{\sigma'=-1}^{1}\langle\Phi_{j'}|\mu_{\rm m}^{(1,\sigma')}(S_1,S_0;\rho)|\Phi_{j''}\rangle\left[(c_{k'}^{(+)})^*c_{k''}^{(+)}\begin{pmatrix}J''&1&J'\\K''&\sigma'&-K'\end{pmatrix}\right.$$
$$+(c_{k'}^{(+)})^*c_{k''}^{(-)}\begin{pmatrix}J''&1&J'\\-K''&\sigma'&-K'\end{pmatrix}+(c_{k'}^{(-)})^*c_{k''}^{(+)}\begin{pmatrix}J''&1&J'\\K''&\sigma'&K'\end{pmatrix}\left.+(c_{k'}^{(-)})^*c_{k''}^{(-)}\begin{pmatrix}J''&1&J'\\-K''&\sigma'&K'\end{pmatrix}\right]. \quad (15)$$

Here, the quantities in parentheses are $3j$-symbols,

$$\mu_{\rm m}^{(1,\pm1)}(S_1,S_0;\rho)=[\mp\mu_b^{(0)}(S_1,S_0;\rho)+i\mu_c^{(0)}(S_1,S_0;\rho)]/\sqrt{2},$$
$$\mu_{\rm m}^{(1,0)}(S_1,S_0;\rho)=\mu_a^{(0)}(S_1,S_0;\rho), \quad (16)$$

and the coefficients $c_k^{(\pm)}$ are the Szalay–Lane coefficients.[30]

To simulate the spectrum it is necessary to convert the line strength $S(f\leftarrow i)$ to the relative integrated absorption coefficient $I(f\leftarrow i)$. We assume a Maxwell–Boltzmann population distribution for the $G_4$ toluenes ($d_1$ and $d_2$), and separate such distributions for the $A$ and $E$ nuclear spin modifications of the $G_{12}$ toluenes ($d_0$ and $d_3$).[2,3,7,8,24,32] The relative intensities are given by

$$I(f\leftarrow i)\propto e^{-(E_i-E_i^0)/kT}S(f\leftarrow i), \quad (17)$$

where $E_i$ is the lower state energy and $E_i^0$ is the energy zero for the distribution to which the $i$th state belongs; this was the $(J,K,K_i)=(0,0,0)$ level except for the $G_{12}$ $E$-state distributions, for which it was (0,0,1). The choice of 0.5 K for the temperature $T$ led to a good reproduction of the experimental spectra.

The rotational and torsional selection rules for the forbidden $a$-type bands of toluene can be understood by considering the dependence of the electronic transition moment on the torsional angle.[7] The dipole moment components $\mu_a$, $\mu_b$, and $\mu_c$ have symmetries $A_1'$, $A_1''$, and $A_2''$ in the $G_{12}$ molecular symmetry group, and the species of the $S_0$ and $S_1$ states of toluene are $A_1'$ and $A_1''$. From these results we see that $\mu_\alpha^{(0)}(S_1,S_0;\rho)$ has symmetry $A_1''$, $A_1'$, and $A_2'$ as $\alpha$ is $a$, $b$ or $c$, respectively. Using the facts that the function $\cos(6n+3)\rho$ transforms as $A_1''$, $\cos 6n\rho$ transforms as $A_1'$, and $\sin(6n+6)\rho$ transforms as $A_2'$ (where $n$ is a non-negative integer), we can write [see Eq. (6) of Ref. 7],

$$\mu_a^{(0)}(S_1,S_0;\rho)=M_3^a\cos 3\rho+M_9^a\cos 9\rho+\cdots, \quad (18)$$

$$\mu_b^{(0)}(S_1,S_0;\rho)=M_0^b+M_6^b\cos 6\rho+M_{12}^b\cos 12\rho+\cdots, \quad (19)$$

and

$$\mu_c^{(0)}(S_1,S_0;\rho)=M_6^c\sin 6\rho+M_{12}^c\sin 12\rho+\cdots. \quad (20)$$

The values of $M_3^a$, $M_0^b$, and $M_6^b$ were determined to be 0.0206, 0.0509, and $-0.0004$ atomic units, respectively, from state-averaged-CASSCF (Ref. 33) calculations of the

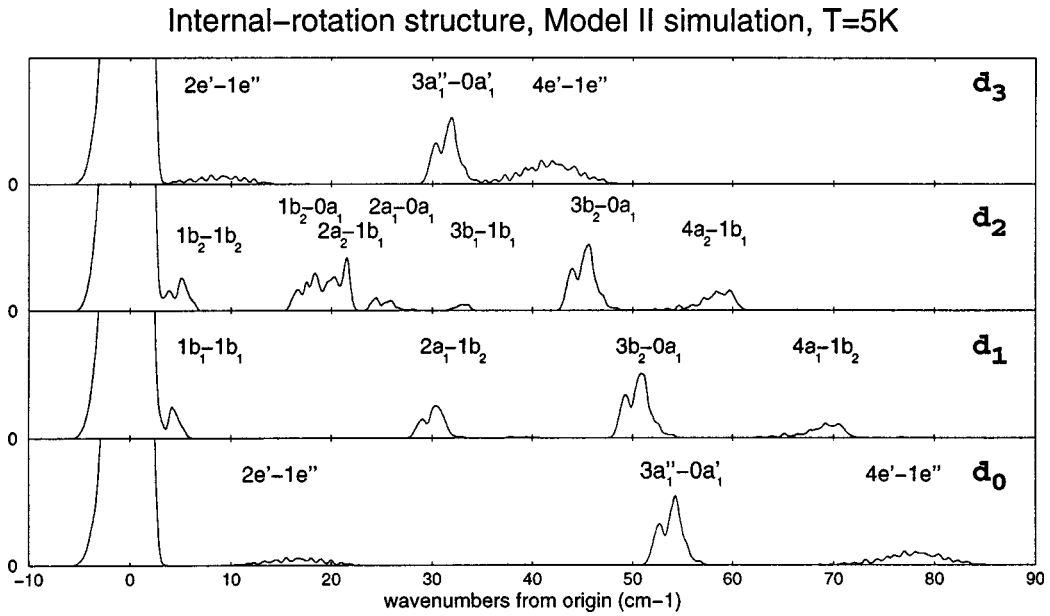


FIG. 2. Simulated spectra of the $S_1-S_0$ internal-rotation structure of (from bottom to top) toluene-$d_0$, -$d_1$, -$d_2$, and -$d_3$, with $(K_i'-K_i'')$ labels. The simulation uses $T=5$ K , $J_{\max}=15$, linewidth $=0.5$ cm$^{-1}$, and the fitted parameters for Model II. The ratio of the peak intensity of the origin band to that of the 3–0 band is 26, 31, 41, and 36, respectively, for the $d_0$, $d_1$, $d_2$, and $d_3$ isotopomers.

three $\mu_\alpha^{(0)}(S_1,S_0;\rho)$ at two $\rho$ values (eclipsed and staggered), using the MOLPRO94 (Ref. 34) program system. Thus, we neglect all $M_n^\alpha$ having $n\geqslant 6$ and in Eqs. (18)–(20) only the parameters $M_3^a$ and $M_0^b$ are considered to be nonvanishing. If *all* dependence on the torsional angle $\rho$ were neglected (i.e., if $M_3^a$ were also neglected) then only $\mu_b^{(0)}(S_1,S_0)$ would be nonvanishing with $\Delta K_i=0$; such bands would have *b*-type rotational structure. Allowing for the dependence of $\mu_\alpha(S_1,S_0)$ on $\rho$ by including $M_3^a$ means that in addition there can be forbidden torsional bands with $\Delta K_i=3$ [$\Phi_{\text{tor}}^{(+)}\leftrightarrow\Phi_{\text{tor}}^{(+)}$ and $\Phi_{\text{tor}}^{(-)}\leftrightarrow\Phi_{\text{tor}}^{(-)}$] having *a*-type rotational structure.

## IV. RESULTS

### A. Internal-rotation structure

The internal-rotation structure in the $S_1-S_0$ spectrum of toluene-$d_0$,[2,3,7] $d_3$,[7] and $d_1$ and $d_2$ (Ref. 9) are known; in Fig. 2 we show the final simulated spectra which closely match the appearance of the experimental spectra.

The initial *ab initio* spectra, using either internal-rotation Model I or II, were qualitatively in agreement with experiment, but there were band position errors of up to 8 cm$^{-1}$ due largely to errors in the internal-rotation potential parameters. From our simulated spectra we were able to estimate more accurately the position of the origin of each of the observed bands; formerly these were estimated only as band maximums or midpoints. We then proceeded to the least-squares fitting (see Appendix) of 16 of the internal-rotation band origins observed for the four isotopomers. We assigned a weight of 50 to the $d_0$ $1-1$ band position, because we knew it 50 times more accurately than the others due to our rotational structure fitting.

Results for the band origins (both experimental and calculated) are presented in Table III. Both Models I and II give satisfactory fits to the data, and the resulting potential parameter values match those found in previous $S_1-S_0$ internal-rotation-structure studies[2,7,9] to within 2 cm$^{-1}$.

### B. Rotational structure

Our experimental spectra of the origin bands are presented in Fig. 3 (toluene-$d_0$) and Fig. 4 ($d_1$ and $d_2$), each sandwiched between the best simulated spectra from fittings with Models I (above) and II (below).

First, note that the $d_1$ and $d_2$ spectra are nearly identical, but that the $d_0$ spectrum has twice as many lines. This is due to the additional presence of the 1–1 band in the $d_0$ spectrum, which has not been cooled away. This is a clear experimental demonstration of the independent existence of a second nuclear-spin modification of $G_{12}$-symmetry toluene. The $d_1$ and $d_2$ toluenes, having only $G_4$ symmetry, do not have such $A-E$ nuclear spin modifications, and hence produce only 0–0 bands at 0.5 K. The 0–0 band is almost identical in all three spectra, and hence the deuteroisotopomer spectra were helpful in assigning the rotational structure of the toluene-$d_0$ spectrum.

Also noticeable in the experimental spectra, shifted 1–2 cm$^{-1}$ to the blue, are faint peaks due to the complex of toluene with an atom from the helium carrier gas. The roughly 2 cm$^{-1}$ shift agrees with that observed for the helium–benzene complex many years ago.[35]

Using our initial *ab initio* rotational structure spectra and intermediate fits, we could assign most of the lines in these three spectra, although we do not have individual line resolution. The rotational line positions are available from the authors on request. The most obvious discrepancy between the experimental and pure *ab initio* spectra was the shift of

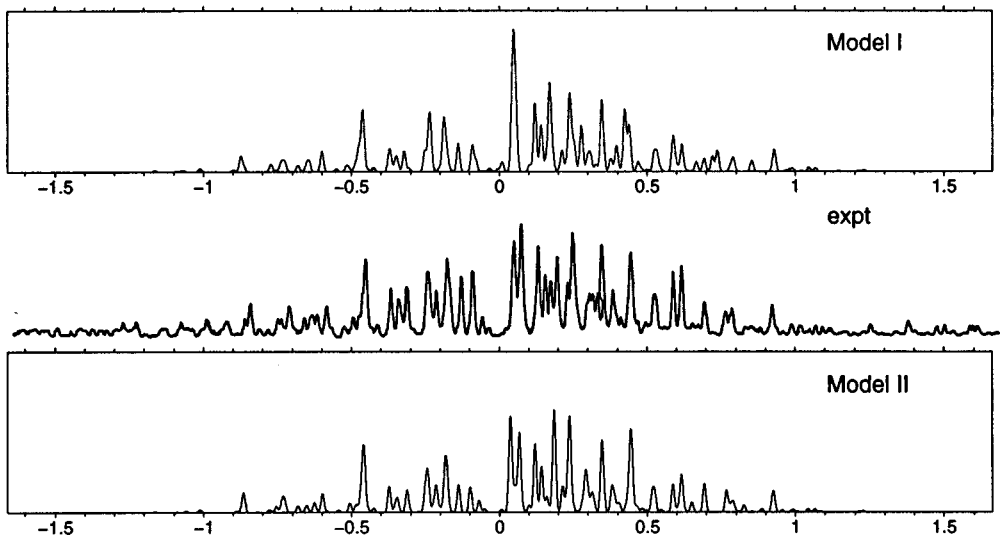


FIG. 3. Experimental (middle trace) and simulated spectra of the rotational structure of the $S_1-S_0$ origin band of toluene-$d_0$, centered at 37 476.56 $cm^{-1}$. The simulations use $T = 0.5$ K, $J_{max} = 8$, linewidth = 0.012 $cm^{-1}$, and the fitted parameters for each internal-rotation model.

the 1–1 band relative to the 0–0 band in the $d_0$ spectrum. We performed fittings to 93 lines in the $d_0$, $d_1$, and $d_2$ spectra (43, 26, and 24 lines, respectively). From the resulting simulations, we obtain an excellent reproduction of the experimental spectra (with very good relative intensities) for all but the Model I simulation of the $d_0$ spectrum (top spectrum of Fig. 3). The simple model has difficulties reproducing the 1−1 band, but not the 0−0 band. The root-mean-square errors were 0.0050 $cm^{-1}$ for Model I and 0.0026 $cm^{-1}$ for Model II. We found that we could achieve an rms deviation of 0.0028 $cm^{-1}$ for Model I when we included $V_6(S_1)$ in the fit, but that $V_6(S_1)$ almost doubled in size and produced up to 5 $cm^{-1}$ errors in the internal-rotation structure; this is unacceptable.

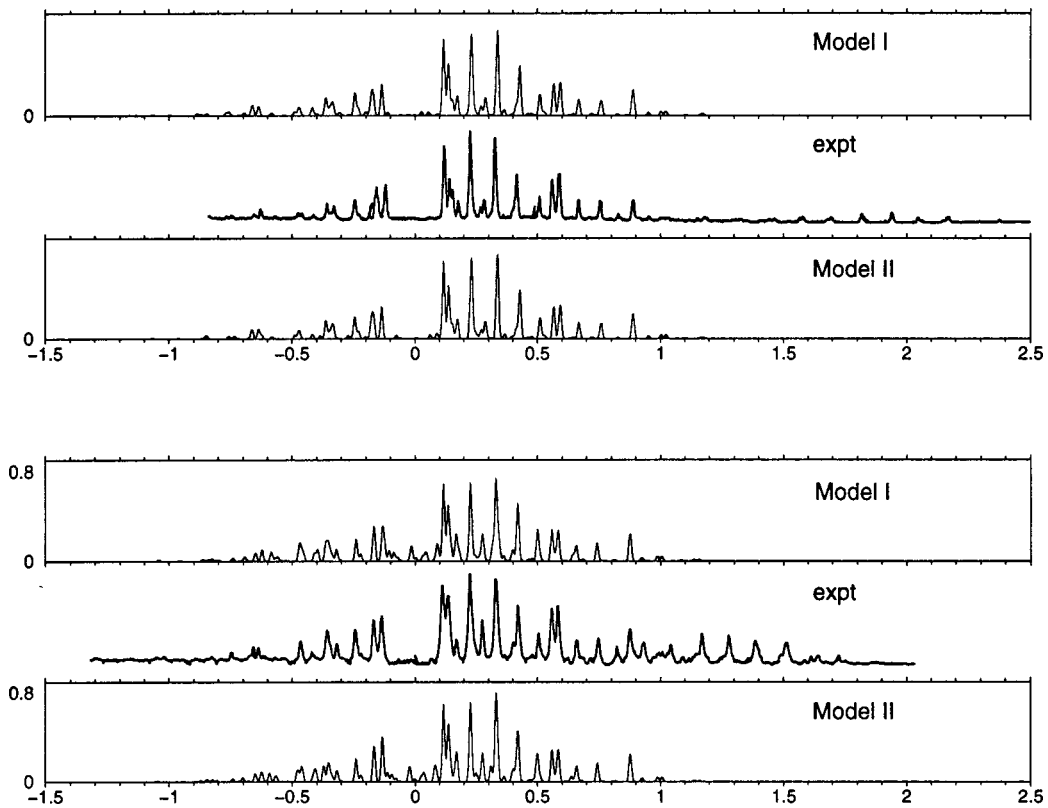


FIG. 4. Experimental and simulated spectra of the rotational structure of the $S_1-S_0$ origin band of toluene-$d_1$ and -$d_2$. The experimental spectra are the 2nd ($d_1$, centered at 37 479.84 $cm^{-1}$), and 5th ($d_2$, centered at 37 487.33 $cm^{-1}$) from the top. The simulations use $T = 0.5$ K, $J_{max} = 8$, linewidth = 0.012 $cm^{-1}$, and the fitted parameters for each internal-rotation model.

The spectral fitting produced values for the geometry and potential parameters which appear in Tables I and II; the Model II result with its fitted parameters is an accurate description of the internal-rotation in toluene.

## V. SUMMARY

The rotational structure in the origin band of the $S_1-S_0$ fluorescence excitation spectra of three isotopomers of toluene has been measured at 0.012 $cm^{-1}$ resolution and a rotational temperature of 0.5 K using a pulsed beam apparatus. Simulations using a minimum energy path model that includes the dependence of the geometrical parameters on the torsional angle $\rho$ give very good fits to both the internal-rotation structure and rotational structure in the spectra, whereas the simple model that neglects this $\rho$-dependence is not satisfactory for fitting the rotational structure of internal-rotation-excited bands. Final geometry parameters are obtained from the fitting for toluene in both the $S_0$ and $S_1$ states, and the resulting geometries for ground and excited-state toluene are the most accurate to date.

## ACKNOWLEDGMENTS

We thank David Borst and David Pratt of the University of Pittsburgh for fruitful discussions. This work was supported in part by the Office of Basic Energy Sciences of the U. S. Department of Energy, by the Deutsche Forschungsgemeinschaft, and by the Fonds der Chemischen Industrie.

## APPENDIX

Generally, the internal-rotation structure gives information about the methyl group geometry and the internal-rotation potential function, while the rotational structure gives information about the overall molecular size. We chose to make the fitting of the internal-rotation structure separately from the fitting to the rotational structure, and to make these fittings in a successive way.

### 1. The parameters varied and the constraints

For the internal-rotation potential function, see Eqs. (1) and (2), we could not determine individual isotopomer values of $V_6$ for a given electronic state and so we constrained the values of $V_6$ for the deuterated versions to have the following fixed relation to the value of $V_6$ for the $d_0$ version:

$$V_6(d_n)=(1-0.043n^{1/2})V_6(d_0). \tag{A1}$$

This formula fits our CASSCF data rather well and is in reasonable accord with an empirical rule for methyl perdeuteration.[1] While we could in this way determine $V_6(d_0)$ for the $S_1$ excited state we could not determine it for the $S_0$ ground state and so we held its value fixed at the CASSCF value of $-3.0$ $cm^{-1}$. For the unsymmetrical isotopomers all $V_2$ terms were varied; the $V_4$ terms did not appreciatively improve our fits to the spectra, and so in the light of our CASSCF results we constrained $V_4 = 0$ in all cases.

Obviously there is not enough data to make a complete geometry determination and it was necessary to have some constraints. For both the $S_0$ and $S_1$ states we took the phenyl $R_{CH}$ bond lengths to be fixed at 1.084 Å,[36] and we kept the angles $\theta_{7,2,1}$ and $\theta_{8,3,4}$ fixed at their CASSCF values. For the other geometry parameters we started from the CASSCF values and then adjusted combinations of them using the parameters $K_T$, $K_R$, $K_M$, and $K_P$ (defined below); these scaling parameters were the parameters that we actually varied in the least squares fitting, and they initially had the value unity.

The parameter $K_T$ is used only in Model II fits and simultaneously scales the methyl tilt parameters $\gamma$ and $\delta$,

$$K_T=\gamma/\gamma^{CASSCF}=\delta/\delta^{CASSCF}. \tag{A2}$$

TABLE IV. Result of fitting to the internal-rotation structure of the $S_1-S_0$ transition, given as shifts from the (0–0) band origin ($cm^{-1}$).

| Isotopomer | Transition | I, CASSCF | II, CASSCF | I, LSQ | II, LSQ | Expt[a] |
|---|---|---|---|---|---|---|
| $PhCH_3$ | $1e''-1e''$ | −0.05 | −0.30 | −0.21 | −0.22 | −0.22 |
| | $2e'-1e''$ | 16.6 | 15.4 | 15.1 | 15.0 | 15.2 |
| | $3a_1''-0a_1'$ | 56.7 | 53.9 | 53.5 | 53.3 | 53.6 |
| | $4e'-1e''$ | 85.1 | 80.2 | 78.8 | 78.5 | 78.2 |
| $PhCH_2D$ | $1b_1-1b_1$ | 2.2 | 2.2 | 3.7 | 3.7 | 3.7 |
| | $2a_1-1b_2$ | 21.4 | 20.7 | 29.8 | 29.7 | 29.8 |
| | $3b_2-0a_1$ | 47.5 | 45.9 | 49.7 | 49.9 | 49.6 |
| $PhCHD_2$ | $1b_2-1b_2$ | 3.2 | 3.2 | 4.6 | 4.6 | 4.6 |
| | $1b_2-0a_1$ | 10.8 | 10.7 | 17.7 | 17.5 | 17.7 |
| | $2a_2-1b_1$ | 16.2 | 15.7 | 21.1 | 21.0 | 20.7 |
| | $2a_1-0a_1$ | 17.9 | 17.6 | 24.9 | 24.8 | 25.0 |
| | $3b_1-1b_1$ | 28.7 | 27.6 | 33.0 | 33.0 | 33.3 |
| | $3b_2-0a_1$ | 40.4 | 39.3 | 44.5 | 44.6 | 44.2 |
| | $4a_2-1b_1$ | 57.5 | 55.6 | 59.0 | 59.4 | 59.2 |
| $PhCD_3$ | $2e'-1e''$ | 8.3 | 7.9 | 7.4 | 7.6 | 7.5 |
| | $3a_1''-0a_1'$ | 32.0 | 31.1 | 30.7 | 30.9 | 31.2 |
| rms error | | 4.3 | 4.3 | 0.25 | 0.22 | |

[a]Our determination from previously published spectra; estimated uncertainty is 0.5 $cm^{-1}$.

The parameter $K_R$ simultaneously scales the bond lengths $R_{C1C12}$ and $R_{C1C4}$,

$$K_R = R_{1,12}/R_{1,12}^{CASSCF} = R_{1,4}/R_{1,4}^{CASSCF}. \quad (A3)$$

The $K_M$ and $K_P$ parameters scale the ''width'' of the methyl (M) or phenyl (P) groups by scaling perpendicular distances $R \sin\theta$, rather than the appropriate $R$ or $\theta$ which we found to be strongly correlated. We did this by scaling angles using $K_M$ and $K_P$, and by scaling bond lengths using $K_M^R$ and $K_P^R$ where

$$K_M^R = (1 - 2\alpha \cot\alpha + [2\alpha \cot\alpha]K_M)^{1/2} \quad (A4)$$

with $\alpha$ taken to be 69°, and

$$K_P^R = (1 - 2\alpha \cot\alpha + [2\alpha \cot\alpha]K_P)^{1/2} \quad (A5)$$

with $\alpha$ taken to be 59.5°. Equations (A4) and (A5) are constraints that arise from scaling appropriate $R$ and $\sin\theta$ equally. The angle scaling is defined by

$$K_M = \beta_{13,12,1}/\beta_{13,12,1}^{CASSCF} \quad (A6)$$

and

$$K_P = \theta_{2,1,6}/\theta_{2,1,6}^{CASSCF} = \theta_{3,4,5}/\theta_{3,4,5}^{CASSCF}. \quad (A7)$$

The bond lengths are scaled according to

$$K_M^R = R_{12,13}/R_{12,13}^{CASSCF} \quad (A8)$$

and

$$K_P^R = R_{1,2}/R_{1,2}^{CASSCF} = R_{3,4}/R_{3,4}^{CASSCF}. \quad (A9)$$

It turned out that $K_T(S_0)$ was indeterminate, $K_M(S_0)$ was determinable only from the internal-rotation structure, and $K_P$ and $K_R$ only from the rotational structure.

### 2. The fitting procedure

For Model I (in which the geometrical parameters were not allowed to vary with $\rho$) our procedure was as follows: We first made a seven parameter fit to the internal-rotation structure in the spectra of all four isotopomers, then an eight parameter fit to the rotational structure of the origin bands of toluene-$d_0$, $d_1$, and $d_2$, and finally we re-adjusted the four $V_2$ parameters in a refitting to all the internal-rotation structure. For Model II (in which the geometrical parameters were allowed to vary with $\rho$) the procedure was the same except for the addition of the $K_T(S_1)$ parameter in the first two fittings. In Table IV we indicate the parameters that were varied in each of the fittings and their final values.


[1] W. A. Kreiner, H. D. Rudolph, and B. T. Tan, J. Mol. Spectrosc. **48**, 86 (1973).
[2] P. J. Breen, J. A. Warren, E. R. Bernstein, and J. I. Seeman, J. Chem. Phys. **87**, 1917 (1987).
[3] J-I. Murakami, M. Ito, and K. Kaya, Chem. Phys. Lett. **80**, 203 (1981).
[4] J. B. Hopkins, D. E. Powers, and R. E. Smalley, J. Chem. Phys. **72**, 5039 (1980).
[5] J. B. Hopkins, D. E. Powers, S. Mukamel, and R. E. Smalley, J. Chem. Phys. **72**, 5049 (1980).
[6] R. D. Gordon and J. M. Hollas, Chem. Phys. Lett. **164**, 255 (1989).
[7] R. A. Walker, E. Richard, K-T. Lu, E. L. Sibert, and J. C. Weisshaar, J. Chem. Phys. **102**, 8718 (1995).
[8] Z-Q. Zhao, C. S. Parmenter, D. B. Moss, A. J. Bradley, A. E. W. Knight, and K. G. Owens, J. Chem. Phys. **96**, 6362 (1992).
[9] W. Siebrand, M. Z. Zgierski, F. Zerbetto, M. J. Wójcik, M. Boczar, T. Chakraborty, W. G. Kofron, and E. C. Lim, J. Chem. Phys. **106**, 6279 (1997).
[10] H. D. Rudolph, H. Dreitzler, A. Jaeschke, and P. Wendling, Z. Naturforsch. Teil A **22**, 940 (1967).
[11] D. Cavagnat and J. Lascombe, J. Mol. Spectrosc. **92**, 141 (1982).
[12] C. Lapouge and D. Cavagnat, J. Phys. Chem. A **102**, 8393 (1998).
[13] C. Zhu, H. G. Kjaergaard, and B. R. Henry, J. Chem. Phys. **107**, 691 (1997).
[14] H. G. Kjaergaard, D. M. Turnbull, and B. R. Henry, J. Phys. Chem. A **101**, 2589 (1997).
[15] H. G. Kjaergaard, D. M. Turnbull, and B. R. Henry, J. Phys. Chem. A **102**, 6095 (1998).
[16] C. M. Pal, P. K. Panja, S. Bala, and P. N. Ghosh, J. Mol. Struct. **189**, 287 (1988).
[17] L. Anastasakos and T. A. Wildman, J. Chem. Phys. **99**, 9453 (1993).
[18] D. Gorse, D. Cavagnat, M. Pesquer, and C. Lapouge, J. Phys. Chem. **97**, 4262 (1993).
[19] D. Cavagnat, L. Lespade, and C. Lapouge, J. Chem. Phys. **103**, 10502 (1995).
[20] T. Cvitaš and J. M. Hollas, Mol. Phys. **20**, 645 (1971).
[21] M. A. Leugers and C. J. Seliskar, J. Mol. Spectrosc. **91**, 150 (1982).
[22] M. A. Leugers and C. J. Seliskar, J. Mol. Spectrosc. **91**, 209 (1982).
[23] C. J. Seliskar, M. Heaven, and M. A. Leugers, J. Mol. Spectrosc. **97**, 186 (1983).
[24] H. Ishikawa, O. Kajimoto, and S. Kato, J. Chem. Phys. **99**, 800 (1993).
[25] H. Liu, E. C. Lim, C. Munoz-Caro, A. Nino, R. H. Judge, and D. C. Moule, J. Mol. Spectrosc. **175**, 172 (1996).
[26] H.-J. Werner and P. J. Knowles, J. Chem. Phys. **82**, 5053 (1985).
[27] P. J. Knowles and H.-J. Werner, Chem. Phys. Lett. **115**, 259 (1985).
[28] M. J. Frisch, G. W. Trucks, H. B. Schlegel, P. M. W. Gill, B. G. Johnson, M. A. Robb, J. R. Cheeseman, T. Keith, G. A. Petersson, J. A. Montgomery, K. Raghavachari, M. A. Al-Laham, V. G. Zakrzewski, J. V. Ortiz, J. B. Foresman, J. Cioslowski, B. B. Stefanov, A. Nanayakkara, M. Challacombe, C. Y. Peng, P. Y. Ayala, W. Chen, M. W. Wong, J. L. Andres, E. S. Replogle, R. Gomperts, R. L. Martin, D. J. Fox, J. S. Binkley, D. J. Defrees, J. Baker, J. P. Stewart, M. Head-Gordon, C. Gonzalez, and J. A. Pople, GAUSSIAN 94, Gaussian Inc., Pittsburgh, Pennsylvania, 1995.
[29] A. L. L. East and P. R. Bunker, J. Mol. Spectrosc. **183**, 157 (1997).
[30] V. Szalay and S. Lane, Mol. Phys. **75**, 781 (1992).
[31] P. R. Bunker and P. Jensen, *Molecular Symmetry and Spectroscopy*, 2nd ed. (NRC Research Press, Ottawa, 1998); see http://www.cisti.nrc.ca/cisti/journals/41653
[32] C. Hartmann, M. Joyeux, H. P. Trommsdorff, J.-C. Vial, and C. von Borczyskowski, J. Chem. Phys. **96**, 6335 (1992).
[33] H.-J. Werner and W. Meyer, J. Chem. Phys. **74**, 5794 (1981).
[34] MOLPRO94 is a package of *ab initio* programs written by H.-J. Werner and P. J. Knowles with contributions from J. Almlöf, R. D. Amos, M. J. O. Deegan, S. T. Elbert, C. Hampel, W. Meyer, K. A. Peterson, R. M. Pitzer, A. J. Stone, and P. R. Taylor.
[35] S. M. Beck, M. G. Liverman, D. L. Monts, and R. E. Smalley, J. Chem. Phys. **70**, 232 (1979).
[36] G. Herzberg, *Molecular Spectra and Molecular Structure* (Krieger, Malabar, 1991), Vol. III.